Detecting Faults in Doubly Fed Induction Generator by Rotor Side Transient Current Measurement

Goran Stojčić, Kenan Pašanbegović, and Thomas M. Wolbank, *Member, IEEE*

***Abstract*—The doubly fed induction generator (DFIG) is one of the main technologies at variable speed power generation systems. Reliability and efficiency are key factors to realize the maximum energy output of the renewable resources. Detecting generator faults enables the reduction of risk for unexpected outages and thus high economic losses. Stator winding insulation faults count to one of the most frequent failures in electric machines. Common fault detection methods are based on several additional sensors and hardware what makes the system complex, expensive and also fault-prone. In this paper, a method is proposed and investigated to detect stator winding faults based only on measured signals available from inverter build-in sensors. By rotor-side inverter switching the generator is excited by transient voltage pulses and the current response provides the possibility to extract a fault indicator through a specific signal processing. Measurements on a DFIG test stand prove the methods applicability and accuracy.**

***Index Terms*—Doubly fed induction machine, fault detection, transient excitation, variable speed applications, winding faults.**

NOMENCLATURE

$\underline{v}_R$	Space vector of the rotor voltages in the stator reference frame (p.u.).
i_S, i_R	Space vector of the stator and rotor currents in the stator reference frame (p.u.).
λ_S	Space vector of the stator flux linkages in the stator reference frame (p.u.).
r_R	Rotor resistance (p.u.).
l_l	Leakage inductance (fundamental wave) (p.u.).
$l_{l,t}$	Transient leakage inductance (p.u.).
l_{offset}	Symmetrical part of transient leakage (p.u.).
l_{mod}	Angle-dependent part of transient leakage (p.u.).
y_{offset}	Symmetrical part of inverse of transient leakage (p.u.).
y_{mod}	Angle-dependent part of inverse of transient leakage (p.u.).
τ	Time (p.u.).
ω_R	Angular rotor speed (p.u.).
γ	Angle of asymmetry.
d	Derivative operator.
arg	Argument of complex number.
U, V, W	Machine phase.
α, β	Stator fixed frame quantities.
Subscripts	
$_{I}$, $_{II}$	Index of first, second pulse and measurement.
$_{I-II}$	Quantity of first pulse minus quantity of second pulse
$_{ASP}$	Asymmetry phasor valuese
Superscripts	
*	Complex conjugate value.

Manuscript received October 9, 2013; revised January 17, 2014; accepted January 26, 2014. Date of publication February 26, 2014; date of current version September 16, 2014. Paper 2013-IPCC-780.R1, presented at the 2013 IEEE Energy Conversion Congress and Exposition, Denver, CO, USA, September 16–20, and approved for publication in the IEEE TRANSACTIONS ON INDUSTRY APPLICATIONS by the Industrial Power Converter Committee of the IEEE Industry Applications Society. This work was supported by the Austrian Science Fund (FWF) under Grant P23496-N24.

The authors are with the Department of Energy Systems and Electrical Drives, Vienna University of Technology, 1040 Vienna, Austria (e-mail: goran.stojcic@tuwien.ac.at; kenan.pasanbegovic@tuwien.ac.at; thomas.wolbank@tuwien.ac.at).

Color versions of one or more of the figures in this paper are available online at http://ieeexplore.ieee.org.

Digital Object Identifier 10.1109/TIA.2014.2308366

I. INTRODUCTION

INCREASING power generation based on renewable energy sources has raised the application of doubly fed induction generator (DFIG). Mainly used in wind turbine and pump-storage applications the DFIG has become a key component. The generator may be subject to different sort of failures and unexpected outages and downtime can lead to high economic losses. Thus, condition monitoring of the generator is mandatory to meet the demands of reliable and cost efficient power generation. Identification of electromechanical generator faults already in an early stage is highly appreciated to enable emergency operation and reduce the risk of catastrophic damages. Detecting faults already in their developing state can provide the possibility to react timely and can prevent from complete destruction of generator or entire system. On the other hand the maintenance efforts can also be reduced by detecting the fault in a very early stage. Monitoring sequences can be carried out periodically and the knowledge of machine state is permanently accessible without the need of reduced maintenance intervals or additional sensors and evaluation systems. Much work has been done in academia as well as industry in this topic [1],[3],[4]. However, most of the methods are based on additional sensors, what makes the condition monitoring and fault detection systems extremely expensive and complex [1]. Another drawback is given by the fact that these sensors are also prone to defects and may lead to additional downtimes. Therefore, methods have to be developed based only on electrical machine quantities as stator/rotor current or voltage to reduce the complexity of the monitoring system. In recent time some methods have been published [1]–[13] dealing with the issue of detecting faults only by generator current and voltage signals. Most of these methods are based on frequency analysis by Fourier transform. In [6] and [7] the well known current signature analysis (CSA) is applied to the rotor modulating signals for the detection of

0093-9994 © 2014 IEEE. Personal use is permitted, but republication/redistribution requires IEEE permission.
See http://www.ieee.org/publications_standards/publications/rights/index.html for more information.

stator and rotor related unbalances. The detection is based on the observation of different side band harmonics influenced by the slip frequency. As DFIG operated predominant in transient conditions the classical Fourier transform fails for accurate fault identification. An improvement of these methods can be found in [8] by using wavelet decomposition for power xdensity analysis or the complex wavelets in [1] for rotor fault detection. A method combination of wavelet analysis and frequency sliding is been presented in [10]. In [11] the Wigner-Ville Distribution is used to identify the rotor asymmetry caused frequency components in the current. Recently in [12] artificial neuronal networks (ANN) are proposed for the decision process and classifying different frequencies to faults. A high resolution frequency technique is shown [13] based on the Multiple Signal Classification (MUSIC).

One of the main drawbacks of such methods is given by the need of a minimum slip frequency. This means that operations near the synchronous speed are not covered. Furthermore, all these methods have to deal with the impact of closed-loop drive systems as they arise from open-loop applications.

This work presents a method enabling detection of incipient faults in DFIG based only on the electrical quantities of rotor and stator. The main advantage is given by the usage of only current sensors of the rotor as well stator that are already present in the control system. Exploiting switching transients of the rotor side inverter provides the possibility to develop a fault indicator for detecting fault induced machine asymmetries. As the rotor is excited by short voltage pulses impacts of closed-loop effects are avoided and the signal processing procedure is kept on a low level using only basic mathematical functions. Thus the presented method can be applied to existing systems easily, considering not only floating point but also fixed point operation processors in the control system.

II. Estimation of Transient Leakage Inductance

The main idea is to exploit the machine response to transient excitation. Short voltage pulses applied by inverter switching to machine terminals will evoke a current response which is dominated by the transient leakage inductance. Comparing the current responses of different phases provides the information on machine's state and asymmetries. It has to be mentioned that in the following description a restriction is made to a specific operation state: rotor winding fed by inverter and the stator winding is short-circuited by an external switch. This is a common start up procedure for doubly fed induction generator applications 0.

Assuming now a symmetrical machine, electrical behavior can be written from rotor side as

$$\underline{v}_R = r_R \cdot \underline{i}_R + l_l \cdot \frac{d\underline{i}_R}{d\tau} + \frac{d\underline{\lambda}_S}{d\tau}. \tag{1}$$

An applied voltage phasor $\underline{v}_R$ generated by any of the active inverter output states leads to a transient current change $d\underline{i}_R/d\tau$. This current change is influenced by different parameters. Besides the leakage inductance l_l also the voltage drop $r_R \cdot \underline{i}_R$ as well as the electromotive force (back emf) from the stator $d\underline{\lambda}_S/d\tau$, the dc link voltage and the inverter output state will influence the current change. After applying a voltage step by inverter switching from inactive to any active state the first current reaction will be dominated by the leakage inductance and the back emf. To enable an accurate identification of the leakage inductance the disturbing back emf has to be eliminated. A simple but very effective way is to apply two short voltage pulses of some μs duration with opposite direction. Due to the short pulse duration the back emf as well as the dc link voltage and fundamental-wave current $\underline{i}_S$ can be assumed constant. Within each pulse duration (1) can be set up individually. Elimination of disturbing voltage drops is then realized by subtraction of both pulse equations as shown in (2) (index I for the first and II for the second pulse, respectively). As the excitation is transient the actual leakage inductance is additionally denoted as the transient leakage inductance $l_{l,t}$ which differs from the fundamental-wave leakage inductance

$$\begin{aligned}\underline{v}_{R,I} - \underline{v}_{R,II} &= \overbrace{r_R \cdot \underline{i}_{R,I} - r_R \cdot \underline{i}_{R,II}}^{\approx 0} + l_{l,t} \cdot \frac{d\underline{i}_{R,I}}{d\tau} \\ &\quad - l_{l,t} \cdot \frac{d\underline{i}_{R,II}}{d\tau} + \underbrace{\frac{d\underline{\lambda}_{S,I}}{d\tau} - \frac{d\underline{\lambda}_{S,II}}{d\tau}}_{\approx 0} \\ &= l_{l,t} \cdot \left[\frac{d\underline{i}_{R,I}}{d\tau} - \frac{d\underline{i}_{R,II}}{d\tau}\right]. \end{aligned} \tag{2}$$

Considering now a real machine, faulty or not the transient inductance will no more be a scalar but a spatial complex value $\underline{l}_{l,t}$. This results from the fact that the direction of the voltage difference phasor $\underline{v}_{R,I-II} = (\underline{v}_{R,I} - \underline{v}_{R,II})$ and the current derivative difference phasor $d\underline{i}_{R,I-II}/d\tau = (d\underline{i}_{R,I}/d\tau - d\underline{i}_{R,II}/d\tau)$ will no longer be aligned.

This complex transient leakage inductance can now be portioned into two parts, an '$offset$' part and a 'mod' (modulated) part (3). The scalar offset part l_{offset} represents the symmetrical machine while the complex modulation part $\underline{l}_{\text{mod}}$ the fault induced asymmetries

$$\begin{aligned}\underline{l}_{l,t} &= l_{\text{offset}} + \underline{l}_{\text{mod}} \\ \underline{l}_{\text{mod}} &= l_{\text{mod}} \cdot e^{j2\gamma}. \end{aligned} \tag{3}$$

As given in (2), measuring of the resulting current slope is sufficient to calculate the angular position of the maximum inductance. This can be done if (3) is inserted in (2) and inverted; what leads to (4) with $\underline{y}_{l,t} = 1/\underline{l}_{l,t}$.

The voltage difference phasor $\underline{v}_{R,I-II}$ can be assumed constant during each measurement period. This leads to the simplification $d\underline{i}_{R,I-II}/d\tau \sim \underline{y}_{l,t}$. thus it is clear that observing only the current derivative difference phasor is sufficient for transient leakage inductance estimation. Furthermore, the number of executed mathematical operations in real time is reduced to a minimum, as only current sampling is needed

$$\frac{d\underline{i}_{R,I-II}}{d\tau} = \underline{y}_{l,t} \cdot \underline{v}_{R,I-II} = \left[y_{\text{offset}} + \underline{y}_{\text{mod}}\right] \cdot \underline{v}_{R,I-II}. \tag{4}$$

With this coherence the measured current derivative difference phasor $d\underline{i}_{R,I-II}/d\tau$ can also be portioned as shown in (4).

The offset part is pointing in the direction of the voltage difference phasor $\underline{v}_{R,I-II}$. On the other hand the modulated part now is dependent on the direction of the maximum inductance. Hence, the modulated part of the current derivative difference phasor provides information on machine asymmetries.

If the spatial direction of the excitation (the voltage difference phasor $\underline{v}_{R,I-II}$) is changed to all three phases, three current derivative phasors are obtained, each containing the offset portion y_{offset} as well as the modulated portion y_{mod}. Spatially combining the three phasors, the offset portion is removed as zero sequence component leaving only the part containing the asymmetry information need for fault detection.

Considering a shorted stator with stator and rotor phase axes aligned, and with the transient scenario due to short voltage pulses in the rotor side, than the time derivative of stator and rotor side phase mmf can each be assumed antiparallel with equal or at least proportional magnitude and with the stator side compensating the rotor. As for the fault detection only the asymmetry or spatial modulation of the leakage inductance is important, both time derivatives resulting from a voltage phasor can be assumed equal in the stator fixed frame following (5). However, it has to be stressed that this is valid only for the considerations made above. It is further important to notice that the proportional relation of stator and rotor side current derivative phasors is sufficient to detect the machine asymmetries in both phasors

$$d\underline{i}_{R,I}/dt \propto -d\underline{i}_{S,I}/dt. \tag{5}$$

With this assumption the current derivative difference phasor $d\underline{i}_{R,I-II}/d\tau$ can be replaced by $d\underline{i}_{S,I-II}/d\tau$, leading to the same asymmetry information regarding the transient leakage inductance as given in (4). Stator and rotor side current measurement both provide the information on the machine asymmetries. The following considerations however, focus on rotor side current measurement only.

III. Fault Indicator Calaculation by Signal Processing

As stated in the previous section, by estimating the current derivative difference phasor the transient leakage inductance information of the generator can be determined and used to detect asymmetries. However, to achieve this detection, some specific signal processing steps have to be performed. In a first step the symmetrical portion of $d\underline{i}_{R,I-II}/d\tau$ has to be eliminated. If the voltage pulses $\underline{v}_{R,I}$ and $\underline{v}_{R,II}$ are applied in opposite directions both aligned with one main phase axis, the resulting voltage difference phasor $\underline{v}_{R,I-II}$ is also aligned with the phase axis. This leads to a current derivative difference phasor $d\underline{i}_{R,I-II}/d\tau$ with the offset component $y_{\text{offset}} \cdot \underline{v}_{R,I-II}$ (representing the symmetrical machine) pointing also the phase axis direction. This procedure is repeated for the remaining two phases leading to three current derivative difference phasors each containing the same offset component magnitude. Spatially combining these three phasors to one resulting phasor leads to the offset components being removed as zero sequence component.

The remaining phasor now only depends on the machine's asymmetries and is denoted asymmetry phasor in the following. An illustrative depiction can be found in Fig. 1. As described, the voltage difference phasors $\underline{v}_{R,I-II}$ are each pointing in one main phase direction and are denoted as $\underline{v}_{R,I-II,U}$, $\underline{v}_{R,I-II,V}$ and $\underline{v}_{R,I-II,W}$, respectively. According to (4) the symmetrical portion $y_{\text{offset}} \cdot \underline{v}_{R,I-II}$ is aligned with the voltage difference phasor while the modulated portion $\underline{y}_{\text{mod}} \cdot \underline{v}_{R,I-II}$ points in the direction of minimum inductance. Thus the resulting current derivative difference phasor for each phase $d\underline{i}_{R,I-II,U}/\tau d\underline{i}_{R,I-II,V}/d\tau$ and $d\underline{i}_{R,I-II,W}/d\tau$ direction has a deviation from the main phase direction.

In a real machine even faultless, there are always some inherent asymmetries present. These asymmetries are detectable and separable due to their deterministic behavior leading to modulation of the asymmetry phasor when the inherent asymmetries spatially move. To achieve an accurate fault indicator signal they have thus to be eliminated. The main reasons for inherent asymmetries are given by winding distribution, slotting and anisotropy. The Fast Fourier Transformation (FFT) provides an effective possibility to separate their modulations from the asymmetry phasor signal. It is however necessary to collect a set of asymmetry phasors clearly showing the spatial movement of the different inherent modulations. This collection can be established by a specific measuring sequence as follows. In a first step the voltage pulse sequences are applied to all three main phase directions and by measurement of the current signal and subsequent signal processing the asymmetry phasor is obtained as described above. In the next stage the rotor is moved and the data acquisition is repeated, at least a phasor set for one mechanical period of the modulation must be acquired. As already mentioned, the method is intended for the very first stage of the start-up or black-start operation of variable speed generator systems. Therewith the rotor movement is realized by the turbine or auxiliary equipment. Ensuring a high quality and accurate signal processing and fault indicator generation the asymmetry phasor set representing 256 rotor position values was collected for one mechanical revolution in this investigation.

The spectral content of the machine investigated in this work is given in Fig. 2. As the asymmetry phasors are complex values the resulting spectrum also is of complex nature. As can be seen, several harmonics are visible in the spectrum. The main harmonics are the -6th, $+12$th, ± 18th and ± 36th. The stator of the present machine has 36 stator slots and 3 pole pairs and thus the ± 36th harmonic is related to this parameter. The -6th harmonic results from a combination of magnetic iron core properties and winding distribution and the ± 18th and $+12$th as higher harmonics of the non-sinusoidal winding modulations. Assuming now a stator related fault (e.g., incipient open-circuit fault, turn-to-turn fault) the electromagnetic properties of the stator winding changes and thus also the transient leakage inductance. Considering now a fault at a certain stator position this will induce an asymmetry equal to the number of poles when moving the rotor and thus the excitation direction for one full mechanical revolution. For the investigated machine this will be the -6th harmonic due to 6 poles. So, a fault induced asymmetry will be detectable in this harmonic and will

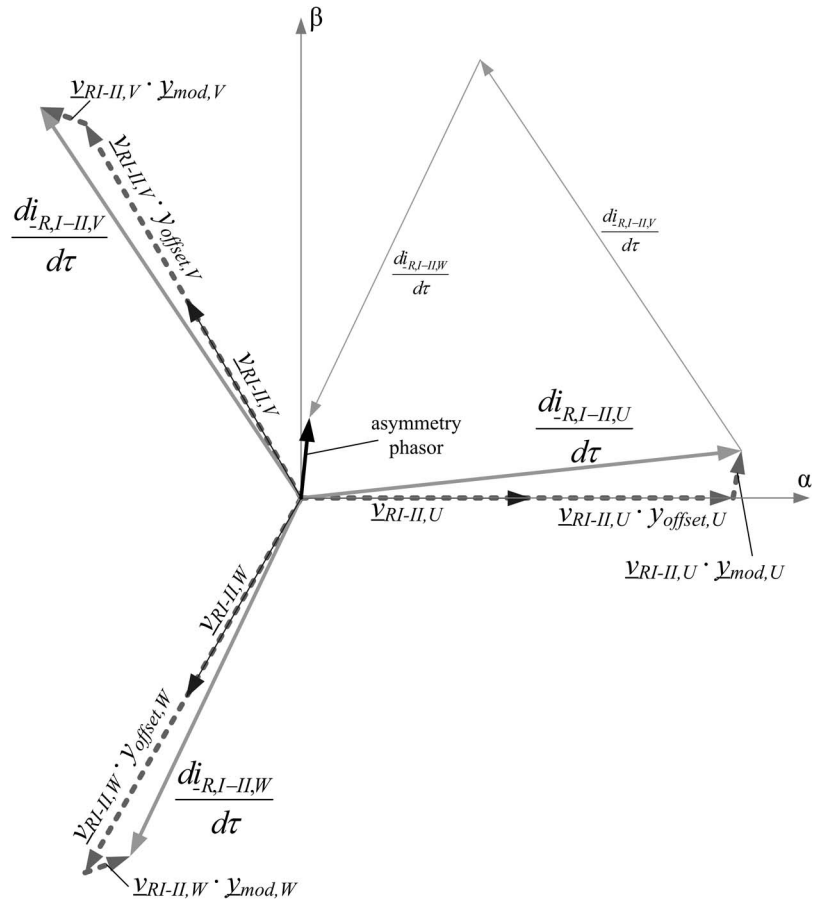

Fig. 1. Space phasor diagram for asymmetry phasor estimation according to transient voltage pulse excitation in all main phase directions.

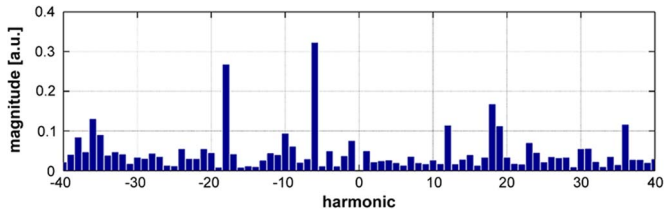

Fig. 2. Harmonic content of the asymmetry phasor for the investigated DFIG und symmetrical conditions (stationary condition).

be denoted as fault indicator. Considering a defect in the rotor, the asymmetry is fixed with the rotor related frame. Thus the harmonic to be observed for such fault cases is the offset. For a clearer presentation of the signal processing Fig. 3 shows a block diagram.

At a fixed rotor position the sequence marked in the dashed rectangle is initiated (with the block denoted "voltage pulses phase U"). At first the voltage pulse sequence in phase U is initiated together with the corresponding measurement of the current response and the calculation of the current derivative difference phasor ("current response measurement"). This is followed by the same procedure repeated in phase V and finally phase W. Once all three current derivative difference phasors are available they are spatially combined according to their phase direction into one resulting phasor ("asymmetry phasor calculation"). There the (symmetrical) offset parts are removed as zero sequence component leaving only the asymmetry portion denoted asymmetry phasor. This asymmetry phasor is stored together with the information on the corresponding rotor position. This sequence is repeated for different rotor positions till enough values for one revolution (e.g.,256) are available.

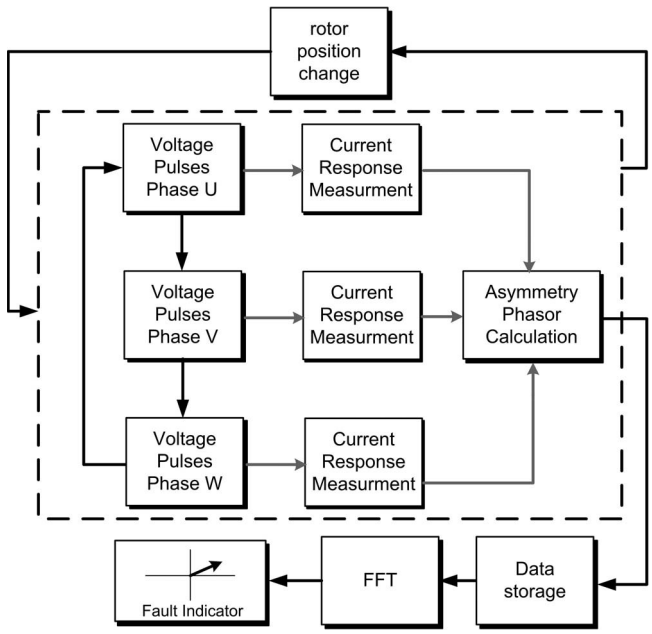

Fig. 3. Block diagram of signal processing for fault indicator generation.

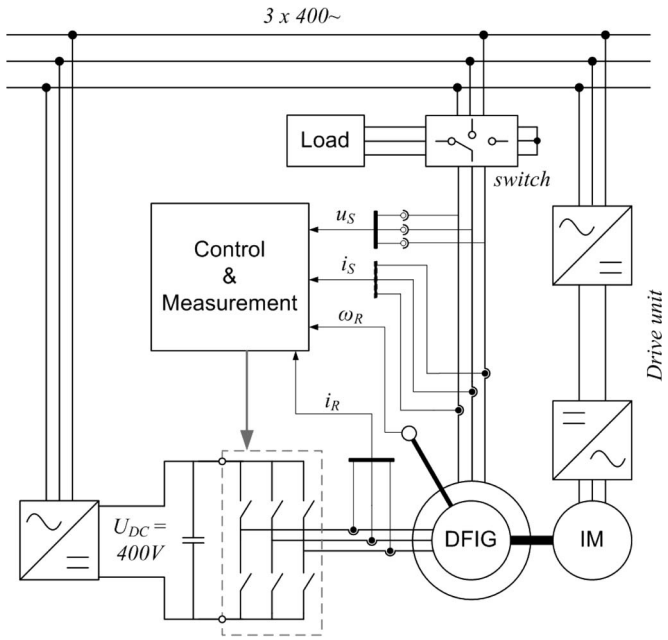

Fig. 4. Scheme of the DFIG test stand.

TABLE I
PARAMETERS OF MACHINE UNDER TEST

NUMBER OF POLES:	P	=	6
NOMINAL VOLTAGE STATOR:	$U_{N,S}$	=	187V
NOMINAL CURRENT STATOR :	$I_{N,S}$	=	14.3A
NOMINAL VOLTAGE ROTOR:	$U_{N,R}$	=	64V
NOMINAL CURRENT ROTOR :	$I_{N,R}$	=	24.8A
NOMINAL EL. FREQUENCY:	F_N	=	50Hz
NUMBER OF STATOR SLOTS:	N_S	=	36
NUMBER OF ROTOR SLOTS:	N_R	=	27

IV. EXPERIMENTAL VERIFICATION BY MEASUREMENTS

A. Test Stand Setup

To prove the methods applicability an experimental test stand was set up as presented in Fig. 4. The test machine (DFIG) is a 6 pole 3.7 kW induction machine with wound rotor and slip ring connectors. The stator has 36 slots and the rotor 27 slots. The parameters of the machine are given in Table I. The stator and rotor windings are specially designed to enable a non destructive simulation of stator and rotor winding faults. For this purpose the winding coils are tapped at several positions enabling the individual connection of different winding turns without winding system destruction. Different fault scenarios can thus be easily realized by simply connecting some of these taps. Disconnection of these joints leads to a healthy, not destructed symmetrical machine again. Through variation of the number of short circuited turn's numerous fault cases can be investigated in a comfortable way.

A voltage source inverter is connected to the slip rings and serves as rotor side inverter. The dc link voltage is 440 V. A variable speed induction machine drive (IM) is operated through an ac-to-ac inverter system and can be controlled by a computer system. This system is the drive unit to realize the rotor movement of the DFIG. The control and measurement system is realized by a computer system programmable under MATLAB/Simulink. The test machine stator can be connected to main supply, short circuited or the machine can be operated under isolated load. This is indicated by a switch in Fig. 4. To ensure the applicability of the proposed method only sensors are used for the calculation of the fault indicator that are also present in standard industrial and power generation systems (stator current and rotor current, stator voltage and shaft speed).

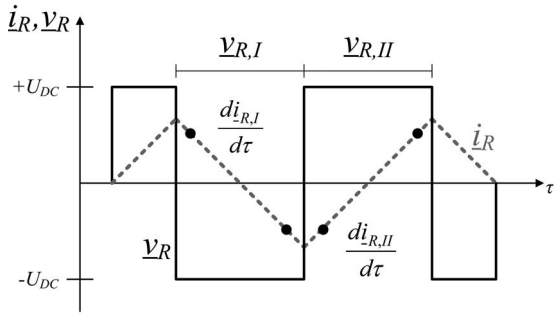

Fig. 5. Voltage pulse excitation sequence in one main phase direction. Black solid line: applied voltage. Gray dashed line: current response. Black dots: current sample instants.

B. Rotor Side Voltage Pulse Generation

The proposed method is based on current response measurement due to short voltage pulse excitation. A simple but very effective way to realize the short voltage pulses is given by inverter switching, changing between different inverter output states. If this procedure is realized with some ten μs duration the assumptions of Section II are met. The voltage pulse excitation is composed of two voltage pulses with their voltage phasors pointing in opposite directions which have to be applied subsequently to eliminate disturbing parameters (resistance and back emf). One possibility to realize this excitation procedure is presented in Fig. 5. The voltage pulses (black solid line) are applied in one main phase direction by changing from positive to negative inverter state in the corresponding phase. As can be seen, the sequence is composed of two short pulses at the beginning and end as well as the two main pulses in the center ($\underline{v}_{R,I}$ and $\underline{v}_{R,II}$). Through this voltage shape a symmetrical excitation (with zero mean voltage) around the operating point is realized (represented by the horizontal axis). The current response is indicated by the gray dashed line. Due to the short pulse duration a linear current response can be assumed. Thus current derivative estimation is realized by two or more sample instants within the pulse duration or by current derivative sensors. In the present work standard industrial current sensors are used. The current derivative is thus measured by two sample instants each within $\underline{v}_{R,I}$ and $\underline{v}_{R,II}$ pulse duration indicated by the black dots in Fig. 5.

As the voltage pulse sequence is only around hundred μs long it can be executed within one cycle of a pulse width modulation (PWM) scheme. For asymmetry phasor calculation the current derivative difference phasors of all main phases are necessary (see also Fig. 3). Thus the pulse sequence depicted is applied in phase U, V and W subsequently. The time duration

between the pulse sequences can be set randomly. To keep the overall measurement procedure short, one PWM cycle is executed between two pulse sequences in different phases in the present work. Regarding the spatial direction of the excitation within the machine it has to be mentioned that the voltage pulses are applied to the rotor through the slip rings. With the movement of the rotor, thus also the angular direction of the exciting voltage pulses with respect to the stator axes is changed.

C. Symmetrical Machine

In a first step the machine was investigated under symmetrical conditions. Therefore, the stator was short-circuited by an external switch and the rotor was slowly moved by the drive unit. This state is common in the very first period of a DFIG during start up 0. The measurements were carried out as described in the previous section.

In Fig. 7 the harmonic content of the asymmetry phasor set obtained by the measurement is presented. As the different asymmetry phasors are obtained from excitation in different spatial positions (equal to the rotor positions), the spectrum contains information on the spatial distribution of the transient leakage inductance along the circumference. The window length is set equal one mechanic revolution. In the upper diagram results are based on rotor current measurement, in the lower diagram based on stator current measurement. All spectra represent the spatial distribution of the transient leakage inductance along the air gap. All the values are given in arbitrary units [a.u.] according to the signal processor internal representation. These arbitrary units are equal to the values used from the digital signal processor (DSP) for quantization according to the ADC values. The values can be associated with the current response and can be converted to ampere per seconds. However, the proposed method is based only on a relative comparison of a singular asymmetry phasor harmonic component between the symmetrical and non-symmetrical case. Hence, a detailed unit conversion is not relevant.

As described in previous section the calculation of the fault indictor can be also executed by using the stator side based current derivative difference phasor $d\underline{i}_{S,I-II}/d\tau$. Thereby the stator current response due to the voltage pulses applied by the rotor-side inverter is measured. The calculation is executed in the very same way but with the current derivative difference phasor $d\underline{i}_{S,I-II,U}/d\tau$, $d\underline{i}_{S,I-II,V}/d\tau$ and $d\underline{i}_{S,I-II,W}/d\tau$ estimated by the stator current measurement. Figs. 6 and 7 are presenting the real part and the harmonic content of the obtained asymmetry phasor set. The machine was operated with zero flux and no load and the stator side was short circuited by an external switch (compare Fig. 4). The drive unit was moving the rotor with 5% of nominal speed and the excitation/measurement was performed till a complete set of asymmetry phasors (ASP) along the mechanical rotor angle was obtained. Comparing the spectra of rotor and stator side measurement, the $+6$th harmonic in the stator related spectrum is more dominant. This modulation is linked with the number of poles (6 for the test machine). The -6th is almost equal in both diagrams.

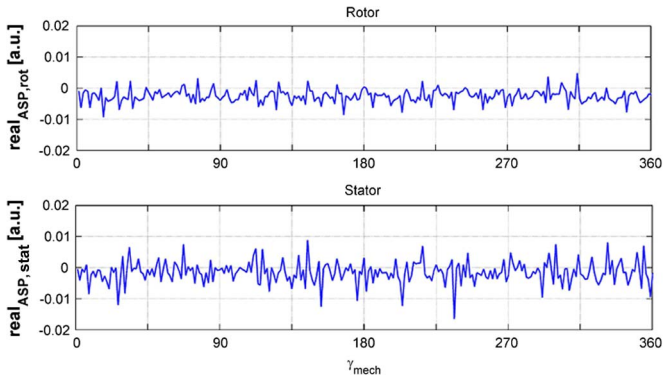

Fig. 6. Real part of the asymmetry phasor set over one mechanical revolution. The current response measurement was performed on the rotor (real$_{\mathrm{ASP,rot}}$, upper diagram) and stator side (real$_{\mathrm{ASP,stat}}$, lower diagram). Machine state: stator short-circuited, symmetrical.

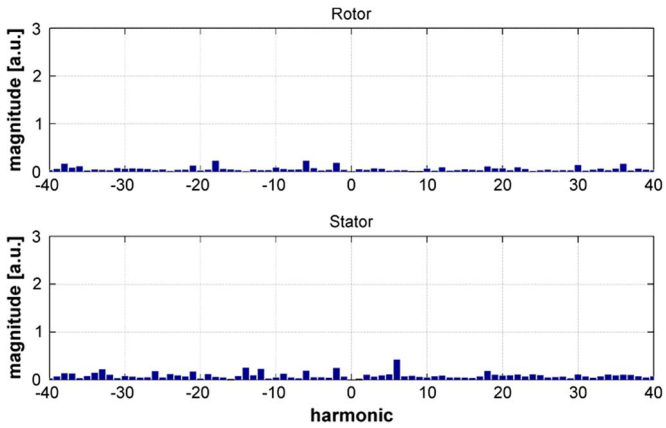

Fig. 7. Harmonic content of the asymmetry phasor set along one mechanical revolution. The current response measurement performed on the rotor (upper diagram) and stator (lower diagram) side. Machine state: stator short-circuited, symmetrical.

D. Stator Related Faults

One of the most frequent faults considering electrical machines are stator related faults. Emulation of such fault cases is realized by connecting the stator winding taps. Thus the resistance value of the short circuited path is $\sim$0. In a first step one coil of phase U was short circuited. The measurement procedure and fault indicator estimation calculations were executed as described for the symmetrical case. To ensure equal conditions the rotor speed was set to 5% nominal value and the stator was short-circuited by an external switch on at the stator terminals (stator current sensors within the short circuit loop). The real portion of the asymmetry phasor set signal and the harmonic content of the signal obtained by this measurement is given in Figs. 8 and 9, respectively. It can be clearly seen that the rotor side real portion signal contains a modulation with a period of 6 corresponding to the mechanical angle γ_{mech}. This can be also observed on the stator side spectrum but with reduced amplitude. In the spectral presentation the difference between stator and rotor side of the -6th harmonic in more visible. These measurements prove that fault detection can be based on the stator or rotor side current measurement as mentioned previously. However, fault indicator calculation is

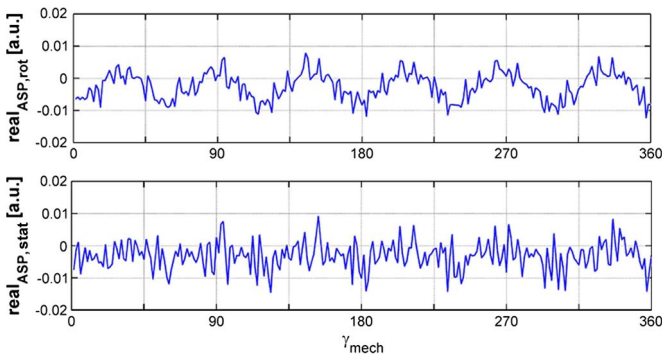

Fig. 8. Real part of asymmetry phasor set. Current response measurement performed on the rotor ($\text{real}_{\text{ASP,rot}}$, upper diagram) and stator side ($\text{real}_{\text{ASP,stat}}$ lower diagram). Machine state: unexcited, one coil in phase U short circuited.

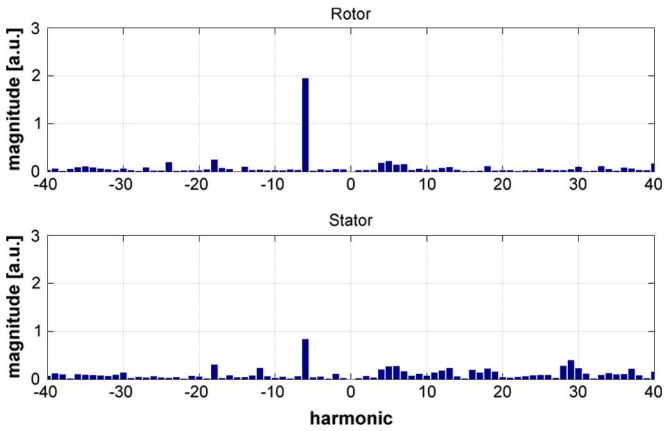

Fig. 9. Harmonic content of the asymmetry phasor set. The current response measurement performed on the rotor (upper diagram) and stator side (lower diagram). Machine state: unexcited, one coil in phase U short circuited.

based on the rotor side due to the dominant increase of the rotor side -6th harmonic and thus an improved signal-to-noise ratio.

E. Stator Fault Detection Accuracy

As the fault indicator obtained from the measurements and calculation is of complex nature, not only asymmetry magnitude (i.e., harmonic content) but also its direction can be identified. The fault indicator can be considered as a phasor in the complex plane pointing in direction of the faulty phase. In Fig. 10 the fault indicator results are shown for several fault cases, 1 (circle), 2 (cross), 10 (square) shorted turns in phase U and 10 shorted turns (star) in phase W. The X is corresponding to the faultless case located in the origin of the complex frame. In addition it must be mentioned that an offset is present even for the faultless machine representing stator fixed asymmetries like anisotropy and measurement equipment (sensors, wiring) imperfections. By pre-commissioning this portion can be eliminated, so done in the present diagram.

By placing a connection between the stator winding taps to short circuit five turns of phase U, an strong asymmetry will be induced leading to a shift of the fault indicator (square) towards phase direction U (gray arrow). The fault indictor is highly displaced from the frame origin indicating a high fault severity. In the next step the fault level is reduced to two turns

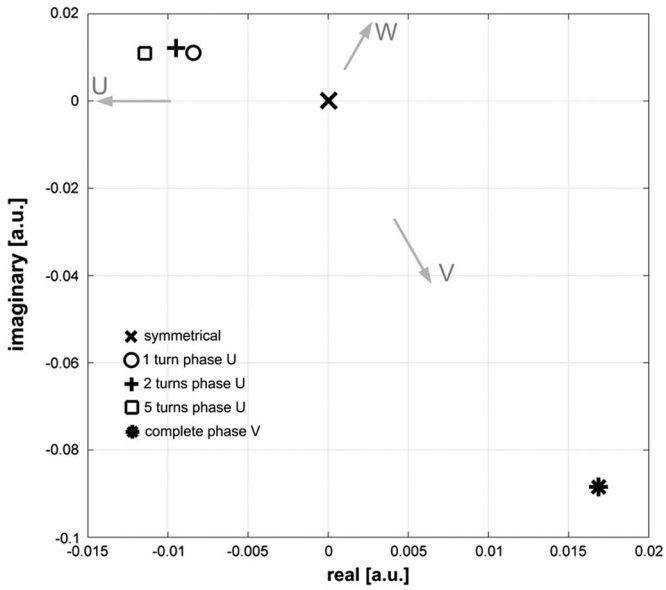

Fig. 10. Fault indicator (offset component) measurement results for faultless case and different stator related fault cases (rotor side measurement).

(cross) and one turn (circle). As can be seen the fault indicator magnitude reduces with decreased fault level. Nevertheless, the fault indictor direction remains almost the same, pointing dominantly in phase direction U.

In the next step the winding taps connection in phase U was removed and a fault in phase V was realized by short circuiting the complete phase. As a consequence, the fault indictor now is shifted to phase V consistent with the realized fault scenario (star). Therewith confusion with phase U faults can be excluded by considering the fault indicator direction. The fault indictor magnitude is strongly increased compared to the magnitude for the single turn faults in phase U.

It has to be stressed that the measurements have only considered occurred faults in one singular phase. As has been shown, the fault indictor magnitude is linked to the fault severity and its angular position to the fault position. Assuming a fault scenario affecting all three phases with equal severity, the fault indictor would then remain near the origin of the complex plane leading to healthy (symmetrical) state interpretation. This issue can be avoided by observing the individual phase values in addition to the calculated asymmetry phasor. In other words the three current derivative difference phasors $d\underline{i}_{R,I-II,U}/d\tau$, $d\underline{i}_{R,I-II,V}/d\tau$, and $d\underline{i}_{R,I-II,W}/d\tau$ can be used as additional fault indicators. However, it has to be stressed, that the symmetrical portion for the healthy case $y_{\text{offset}} \cdot \underline{v}_{R,I-II}$ must be identified in advance through reference measurements and removed by subtraction.

F. Rotor Related Faults

Beside the stator related faults also rotor winding faults count to frequent faults considering wound rotor machines. As the transient leakage inductance is influenced by the stator as well rotor side, also rotor related faults can be identified. Therefore, the fault indictor estimation must be adapted due to the fact

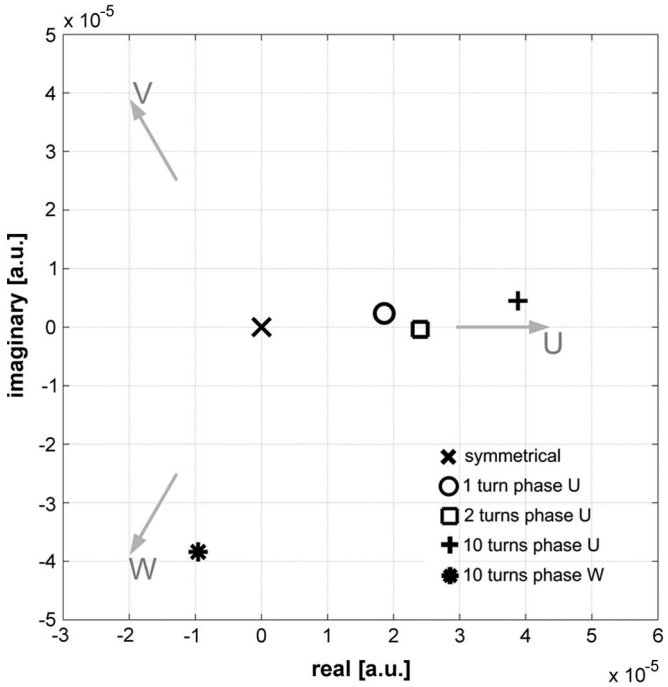

Fig. 11. Fault indicator (−6th harmonic) measurement results for faultless case and different rotor related fault cases (rotor side measurement).

that the excitation is fixed with rotor windings. Assuming a fault in the rotor windings the faulty position is also moving with the rotor. Thus the fault induced harmonic of the fault indicator is not equal the pole pair as for stator related faults but the offset component. So, the measurement procedure and signal processing presented in Fig. 3 remains the same and but the fault indicator is now the offset harmonic component of the spectral content.

Verification of fault detection applicability and accuracy was realized for the rotor related faults by connecting different taps of the rotor winding system. Several fault cases and measurements were performed. In Fig. 11 all the results are presented as end points of the spatial fault indicator in the complex plane. The fault severities and positions were realized similar to the stator fault scenarios. At first, the symmetrical machine was investigated. The stator was short-circuited at the terminals by the external switch (Fig. 4) and the rotor speed was set again to 5% nominal value. The fault indicator result for this symmetrical configuration is located again at the origin of the complex plane (X). In the next step, the very first ten turns of the rotor in phase U were short circuited (cross). Comparing now the fault indicator results of stator and rotor related faults it can be seen that the direction of the fault indicator movement is shifted in opposite direction. In the next step, the fault is reduced stepwise to 2 turns (square) and finally to 1 turn of the rotor winging (circle). As visible, the fault indictor is shifted towards the origin of the complex plane indicating reduced fault levels. Nevertheless, the fault indicator for all three fault cases clearly points in phase direction U and the magnitude is decreasing with lower asymmetry values. In a final fault scenario phase W of the rotor is affected through ten short circuit turns (star). Hence, the direction of the fault indicator points into phase direction W indicating a fault in this phase.

V. Discussion

The proposed fault indicator for stator and rotor related faults has been verified through measurements on a test stand by emulating faults on a special designed test machine. It was shown, that even a single short circuited turn in one phase can be clearly detected. With continuous development of an unbalance (increase of the number of shorted turns) the fault indictor will increase in magnitude towards the affected phase direction. In general, faults usually occur during operation. And it is always desirable to detect the fault in the starting period to have enough time for timely reaction. The presented method in the current state cannot be applied during machine operation as a short circuited stator at the machine terminals is needed. Thus it is limited as a test during start up period. However, further developments and investigations are in progress to realize also online monitoring. First test already show promising results.

VI. Conclusion

The technique presented in this paper allows the detection of stator and rotor related asymmetries in the winding system of doubly fed induction generators. Applying short voltage pulses of some ten μs duration to the machine terminals and measuring the current reaction provides the knowledge of the machine's transient leakage inductance. By a special signal processing procedure a fault indicator is developed to identify stator asymmetries by using the rotor side inverter built-in current sensors only. Asymmetries can be detected with their severity as well as position. A special test stand with a slip ring induction machine having taped winding in stator as well as rotor side and a drive unit was set up to prove the methods applicability and accuracy. The asymmetry emulation was realized by connecting the tapings of the winding at various winding positions. Measurements for different fault scenarios have shown satisfactory results when detecting the fault induced asymmetries.

References

[1] Z. Daneshi-Far, G. A. Capolino, and H. Henao, "Review of failures and condition monitoring in wind turbine generators," in *Proc. XIX ICEM*, 2010, pp. 1–6.

[2] B. Lu, Y. Li, X. Wu, and Z. Yang, "A review of recent advances in wind turbine condition monitoring and fault diagnosis," in *Proc. IEEE PEMWA*, 2009, pp. 1–7.

[3] M. R. Wilkinson, F. Spinato, and P. J. Tavner, "Condition monitoring of generators & other subassemblies in wind turbine drive trains," in *Proc. IEEE SDEMPED*, 2007, pp. 388–392.

[4] Z. Hameed, Y. S. Hong, Y. M. Cho, S. H. Ahn, and C. K. Song, "Condition monitoring and fault detection of wind turbines and related algorithms: A review," *Renew. Sustain. Energy Rev.*, vol. 13, no. 1, pp. 1–39, Jan. 2009.

[5] A. Yazidi, H. Henao, G. A. Capolino, M. Artioli, and F. Filippetti, "Improvement of frequency resolution for three phase induction machine fault diagnosis," in *Conf. Rec. IEEE IAS Annu. Meeting*, 2005, pp. 20–25.

[6] A. Stefani *et al.*, "Doubly fed induction machines diagnosis based on signature analysis of rotor modulating signals," *IEEE Trans. Ind. Appl.*, vol. 44, no. 6, pp. 1711–1721, Nov./Dec. 2008.

[7] A. Stefani, F. Filippetti, and A. Bellini, "Diagnosis of induction machines in time-varying conditions," *IEEE Trans. Ind. Electron.*, vol. 56, no. 11, pp. 4548–4556, Nov. 2009.

[8] J. Cusido, L. Romeral, J. A. Ortega, J. A. Rosero, and A. G. Espinosa, "Fault detection in induction machines using power spectral density in wavelet decomposition," *IEEE Trans. Ind. Electron.*, vol. 55, no. 2, pp. 633–643, Feb. 2008.

[9] I. P. Tsoumas, G. Georgoulas, E. D. Mitronikas, and A. N. Safacas, "Asynchronous machine rotor fault diagnosis technique using complex wavelets," *IEEE Trans. Energy Convers.*, vol. 23, no. 2, pp. 444–459, Jun. 2008.
[10] Y. Gritli, A. Stefani, C. Rossi, F. Filippetti, and A. Chatti, "Doubly fed induction machine stator fault diagnosis under time-varying conditions based on frequency sliding and wavelet analysis," in *Proc. IEEE SDEMPED*, 2009, pp. 1–7.
[11] V. Climente-Alarcon, M. Riera-Guasp, J. Antonino-Daviu, J. Roger-Folch, and F. Vedreno-Santos, "Diagnosis of rotor asymmetries in wound rotor induction generators operating under varying load conditions via the Wigner-Ville Distribution," in *Proc. SPEEDAM*, pp. 1378–1383.
[12] S. Toma, L. Capocchi, and G.-A. Capolino, "Wound-rotor induction generator inter-turn short-circuits diagnosis using a new digital neural network," *IEEE Trans. Ind. Electron.*, vol. 60, no. 9, pp. 4043, 4052, Sep. 2013.
[13] S. H. Kia, H. Henao, and G. A. Capolino, "A high-resolution frequency estimation method for three-phase induction machine fault detection," *IEEE Trans. Ind. Electron.*, vol. 54, no. 4, pp. 2305–2314, Aug. 2007.

Goran Stojčić received the B.Sc. degree in electrical engineering in 2009 and the M.Sc. degree in power engineering in 2011 from Vienna University of Technology, Vienna, Austria, where he is currently working toward the Ph.D. degree.

He is a Project Assistant in the Department of Energy Systems and Electrical Drives, Vienna University of Technology. His special fields of interest are fault detection and condition monitoring of inverter-fed drives.

Kenan Pašanbegović received the B.Sc. degree in electrical engineering and the M.Sc. degree in automation engineering from Vienna University of Technology, Vienna, Austria in 2012 and 2013, respectively.

He is currently with the Department of Energy Systems and Electrical Drives, Vienna University of Technology. His special fields of interest are machine control, fault detection and condition monitoring in inverter-fed drives.

Thomas M. Wolbank (M'99) received the Doctoral degree and the Habilitation (Associate Professor degree) from Vienna University of Technology, Vienna, Austria, in 1996 and 2004, respectively.

Currently, he is with the Department of Energy Systems and Electrical Drives, Vienna University of Technology. He has coauthored more than 100 papers published in refereed journals and international conference proceedings. His research interests include saliency-based sensorless control of ac drives, dynamic properties and condition monitoring of inverter-fed machines, transient electrical behavior of ac machines, and motor drives and their components and their control by the use of intelligent control algorithms.